

Chapter 6

Enhancing the Rate of Spontaneous Emission in Active Core-Shell Nanowire Resonators

6.1 Introduction

Researchers have devoted considerable effort to enhancing light emission from semiconductors and molecules using optical geometries that exhibit high Purcell factors [69]. To effectively enhance the rate of spontaneous emission, one must maximize the quantity of Q/V . This is traditionally achieved by designing dielectric resonators with high quality factors, Q . Although plasmonic nanocavities generally support resonant modes with low quality factors ($Q < 50$), these modes are highly confined to subwavelength mode volumes ($V \ll (\lambda/n)^3$) and can also exhibit very large Purcell factors. It has long been recognized that metal films and nanostructures can enhance the fluorescence of molecules [77, 78] and semiconductors [79, 80], and since then a number of more complex plasmonic nanoparticle and nanoantenna geometries have been employed to modify the spontaneous emission rate [81, 82]. Recently, plasmon-enhanced stimulated emission was demonstrated in two new devices, the spaser (surface plasmon amplification by stimulated emission of radiation) nanolaser [83] and the plasmon laser [84]. Here, we demonstrate an equally dramatic effect on the spontaneous emission rate of inorganic semiconductors in ultra-small mode volume cavities.

In this chapter, we investigate plasmonic core-shell nanowire resonators consisting

of a III-V compound semiconductor heterostructure nanowire core surrounded by an optically thick Ag coating, shown schematically in Figure 6.1. Enhancing the spontaneous emission rate of III-V semiconductors is of particular interest because they have high internal quantum efficiency and an ability to form high-quality heterostructures. We will use a method similar to Chapter 4 to investigate these structures, but now incorporate active III-V semiconductor light emitters into the semiconductor core.

6.2 Theoretical Methods

The semiconductor heterostructure core has an active light emitting region (length L_A , radius a) clad on all sides with a larger band-gap material (length L_C and thin spacer layer thickness s), an Ag coating thickness T , and a total resonator length $L = L_A + 2L_C$ (Figure 6.1). This geometry allows for significant modification of the local density of optical states (LDOS), which describes the available optical eigenmodes for photons at a specific position, orientation, and frequency. The decay rate of excited atoms is proportional to the LDOS. Changing the material and dimensions of the semiconductor core directly modifies the LDOS, and thus controls the radiative emission rate. Furthermore, we take advantage of the modest quality factors in these plasmonic nanostructures ($Q < 50$) to achieve band-to-band spontaneous emission enhancement. We use the boundary element method (BEM) to investigate the LDOS in these structures [62, 85], choosing dimensions of the resonator such that the lowest-order longitudinal resonance overlaps with the emission wavelength of the active material. For this mode, we determine the LDOS, effective mode volume (V_{eff}), quality factor (Q), and enhancements in the total and radiative decay rates (Γ_{tot} and Γ_{rad} , respectively, normalized to decay in vacuum, Γ_0), and the corresponding quantum efficiency $\eta = \Gamma_{\text{rad}}/\Gamma_{\text{tot}}$.

In the BEM, calculations are performed in the frequency domain with the electromagnetic field in each homogeneous region expressed as a function of auxiliary boundary charges and currents. After applying boundary conditions, a set of linear integrals is obtained and solved by discretization. The axial symmetry of core-shell nanowire

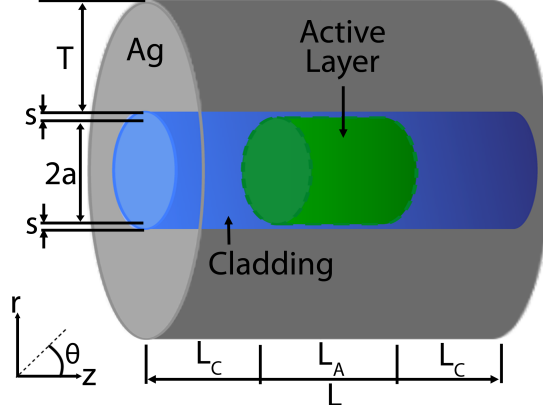


Figure 6.1. Schematic of a plasmonic core-shell nanoresonator. The nanowire core consists of a III-V semiconductor active layer (length L_A and radius a) clad with a wider band-gap III-V semiconductor (segment lengths L_C and spacer thickness s) and coated with Ag (thickness T and total length $L = 2L_C + L_A$).

resonators allows decomposition of the fields into uncoupled azimuthal components m with angular dependence $e^{im\phi}$. This results in an essentially one-dimensional field calculation that is solved with great accuracy. Converged results are found for $m_{\max} = 1$, using values of m defined by

$$m = -m_{\max}, -m_{\max} + 1, \dots, m_{\max} - 1, m_{\max}. \quad (6.1)$$

The dielectric functions of the core and cladding materials are input using tabulated data [34, 86, 87, 88, 89]. Resonant modes are determined by calculating the LDOS ρ for a dipole emitter oriented along a radial direction using the relation

$$\rho = \frac{\omega^2 n}{3\pi^2 c^3} + \frac{1}{2\pi^2 \omega} \text{Im}[E_{\text{ind}}/D], \quad (6.2)$$

where ω is the resonance frequency, c is the speed of light in vacuum, n is the refractive index of the active semiconductor, D is the dipole strength, and E_{ind} is the contribution to the electric field due to scattering at the interfaces and projected along the direction of polarization. The resonance quality factor, Q , is determined

by fitting a Lorentzian lineshape to a plot of ρ vs. ω , and

$$Q = \frac{\omega}{\Delta\omega}, \quad (6.3)$$

where $\Delta\omega$ is the full width at half maximum.

In addition to calculating the LDOS, we determine the spatial near-field electric field intensity (NF $|\mathbf{E}|^2$) profiles of each mode by using plane-wave excitation incident at $\theta = 0^\circ$, polarized along an arbitrary radial direction (see Figure 6.1). The effective mode volume, V_{eff} , is defined as a cylinder with length L_{eff} and radius a_{eff} given by the $1/e$ decay distance of the peak field intensity inside the semiconductor core as $V_{\text{eff}} = \pi a_{\text{eff}}^2 L_{\text{eff}}$. To determine what portion of the decay contributes to radiative emission and absorption, we assume that the compound semiconductor active material has unit internal quantum efficiency in homogeneous bulk materials [90] and calculate the enhancements in the total and radiative decay rates normalized to Γ_0 , the decay rate in vacuum, given by

$$\Gamma_0 = \frac{4}{3} \frac{|D|^2}{\hbar} \left(\frac{\omega}{c}\right)^3. \quad (6.4)$$

The total decay rate, Γ_{tot} , is related to the LDOS ρ as

$$\Gamma_{\text{tot}} = \frac{4\pi^2\omega|D|^2}{\hbar} \rho. \quad (6.5)$$

Finally, the radiative decay rate, Γ_{rad} , is calculated by integrating the far-field Poynting vector for a dipole source (polarized along r) located in the center of the resonator core.

6.3 Modes of Active Core-Shell Nanowire Resonators

Detailed results are presented for three resonators, each composed of a different III-V compound semiconductor active emitter (GaAs, $\text{Al}_{0.42}\text{Ga}_{0.58}\text{As}$, and $\text{In}_{0.15}\text{Ga}_{0.85}\text{N}$).

6.3.1 GaAs-In_{0.51}Ga_{0.49}P-Ag Resonator

We first consider GaAs as an active material with a band gap (emission wavelength) $E_g = 1.424$ eV ($\lambda = 870$ nm), clad with In_{0.51}Ga_{0.49}P, which is lattice matched to GaAs. A thin In_{0.51}Ga_{0.49}P spacer layer is located between the GaAs active region and Ag coating to prevent quenching of excitons located near the metal/semiconductor interface. The lowest-order longitudinal resonance occurs at the proper wavelength for a resonator with dimensions $a = 36$ nm, $s = 6$ nm, $L_A = 100$ nm, $L_C = 25$ nm, and $T = 100$ nm. Figure 6.2 shows contour plots of the LDOS and NF $|\mathbf{E}|^2$ for plane-wave excitation at $\theta = 0^\circ$ as a function of both wavelength and distance along the z -axis at a constant radial position of $r = 5$ nm. It is clear from Figure 6.2 that the mode at $\lambda = 870$ nm has LDOS peaked in the GaAs region of the core. Additional modes are supported at shorter wavelengths, but these do not overlap with the emission wavelength of the active material and do not have the proper symmetry to support large decay rate enhancements. Furthermore, we see from Figure 6.2 that plane-wave excitation at $\lambda = 870$ nm excites the same mode profile, with high fields localized inside the GaAs region. The modes at shorter wavelengths are not excited here because of symmetry.

We also calculate two-dimensional cross sections of the LDOS and NF $|\mathbf{E}|^2$ for the mode at $\lambda = 870$ nm. The LDOS in Figure 6.3b is calculated in the semiconductor core, and illustrates that indeed high LDOS is peaked inside the GaAs region. High intensity is also localized in the thin spacer layer. Plane wave excitation at $\lambda = 870$ nm allows investigation of the electric field localization, and high confinement of the fields in both the radial and longitudinal directions is demonstrated in the two-dimensional NF $|\mathbf{E}|^2$ cross section of Figure 6.3c. The regions of high field intensity in the core correlate to regions of high LDOS, and thus also to large enhancements in the total decay rate. This mode has a moderate quality factor of 45 and an effective mode volume $V_{\text{eff}} = 0.070(\lambda/n)^3$, for $Q/V_{\text{eff}} = 645(\lambda/n)^{-3}$. The radiative decay rate enhancement is calculated for a dipole located in the center of the resonator polarized along the r -direction, and we find $\Gamma_{\text{tot}}/\Gamma_0 = 223$, $\Gamma_{\text{rad}}/\Gamma_0 = 128$, and $\eta = 0.57$.

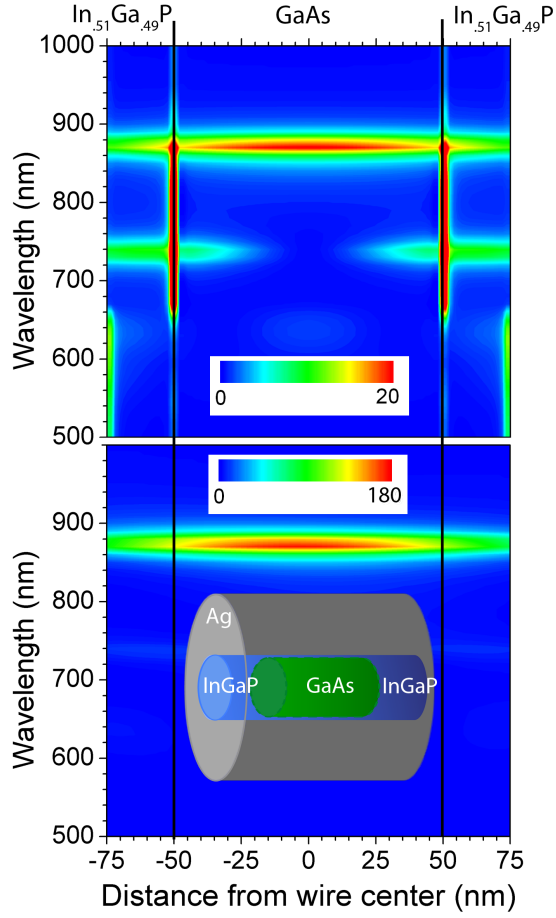


Figure 6.2. Resonant modes for a structure with GaAs active layer ($a = 36$ nm, $L_A = 100$ nm), $\text{In}_{0.51}\text{Ga}_{0.49}\text{P}$ cladding ($s = 5$ nm, $L_C = 25$ nm), and Ag coating thickness $T = 100$ nm. The LDOS (top) and NF $|\mathbf{E}|^2$ (bottom) are calculated at a constant radial position of $r = 5$ nm from the center of the resonator core and along the length of the wire, at wavelengths between $\lambda = 500$ and 1000 nm. The values of LDOS reported are normalized to the LDOS in vacuum. The structure is shown schematically in the inset.

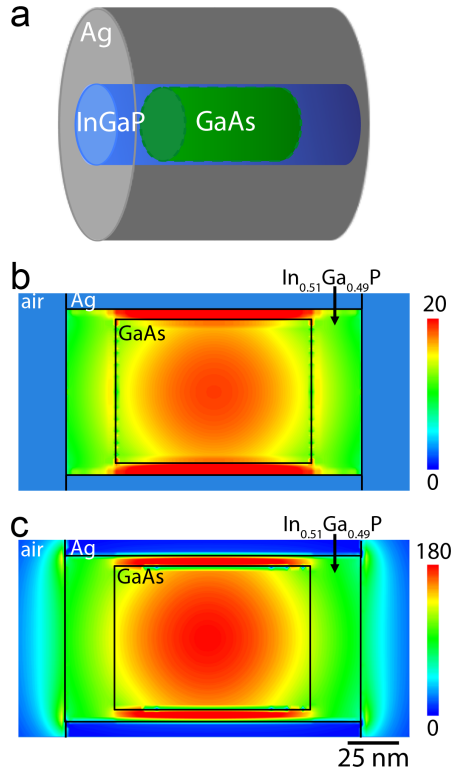


Figure 6.3. (a) Schematic of a GaAs-InGaP-Ag core-shell nanowire resonator with GaAs active layer ($a = 36$ nm, $L_A = 100$ nm), $\text{In}_{0.51}\text{Ga}_{0.49}\text{P}$ cladding ($s = 5$ nm, $L_C = 25$ nm), and Ag coating thickness $T = 100$ nm. Two-dimensional profiles of the (b) LDOS at $\lambda = 870$ nm and (c) $\text{NF } |\mathbf{E}|^2$ cross section for plane-wave excitation at $\lambda = 870$ nm ($\theta = 0^\circ$), the emission wavelength of GaAs, show that both high LDOS and high electric fields are concentrated inside the GaAs active region, in a mode that is highly confined within the semiconductor core.

6.3.2 $\text{Al}_{0.42}\text{Ga}_{0.58}\text{As}-\text{Al}_{0.70}\text{Ga}_{0.30}\text{As}-\text{Ag}$ Resonator

To investigate a smaller structure with modes at shorter wavelengths, we choose $\text{Al}_{0.42}\text{Ga}_{0.58}\text{As}$ as the active material. This alloy has $E_g = 1.95$ eV, emitting at a wavelength of $\lambda = 637$ nm. A ternary alloy with higher Al content, $\text{Al}_{0.70}\text{Ga}_{0.30}\text{As}$, is chosen for the cladding and spacer material, which is an indirect band-gap semiconductor with $E_g = 2.07$ eV. A core-shell nanowire resonator composed of these materials with dimensions $a = 14$ nm, $s = 5$ nm, $L_A = 20$ nm, $L_C = 30$ nm, and $T = 100$ nm has the lowest order longitudinal resonance at $\lambda = 637$ nm. The LDOS and NF $|\mathbf{E}|^2$ mode profiles along the length of the resonator, calculated at a radial position of $r = 5$ nm from the center of the core, are shown in Figure 6.4. Note the twofold increase in LDOS of the lowest order mode as compared to the larger GaAs structure. A plane wave at $\lambda = 637$ nm also excites this mode with a longitudinal profile that matches the LDOS.

The two-dimensional LDOS and NF $|\mathbf{E}|^2$ profiles for the mode at $\lambda = 637$ nm are shown in Figure 6.5. The LDOS profile shows that high LDOS can be found throughout the core, suggesting that the total decay rate will be enhanced for dipole emitters located throughout the semiconductor. The NF $|\mathbf{E}|^2$ profile in demonstrates that even in this smaller structure, fields are highly confined in the semiconductor core with minimal field penetration into the surrounding medium. This mode has $Q = 30$, $V_{\text{eff}} = 0.021(\lambda/n)^3$, and $Q/V_{\text{eff}} = 1435(\lambda/n)^{-3}$, with decay rate enhancement $\Gamma_{\text{tot}}/\Gamma_0 = 460$, $\Gamma_{\text{rad}}/\Gamma_0 = 280$, and $\eta = 0.60$. Comparing these results to the GaAs resonator, we see that the smaller resonator continues to exhibit high modal confinement with an effective mode volume approximately equal to the physical volume of the semiconductor core, and that the lowest-order longitudinal resonance does not sustain much loss in quality factor with decreased dimensions. Thus, the figure of merit Q/V_{eff} more than doubles in this smaller resonator relative to the first example using GaAs, described above.

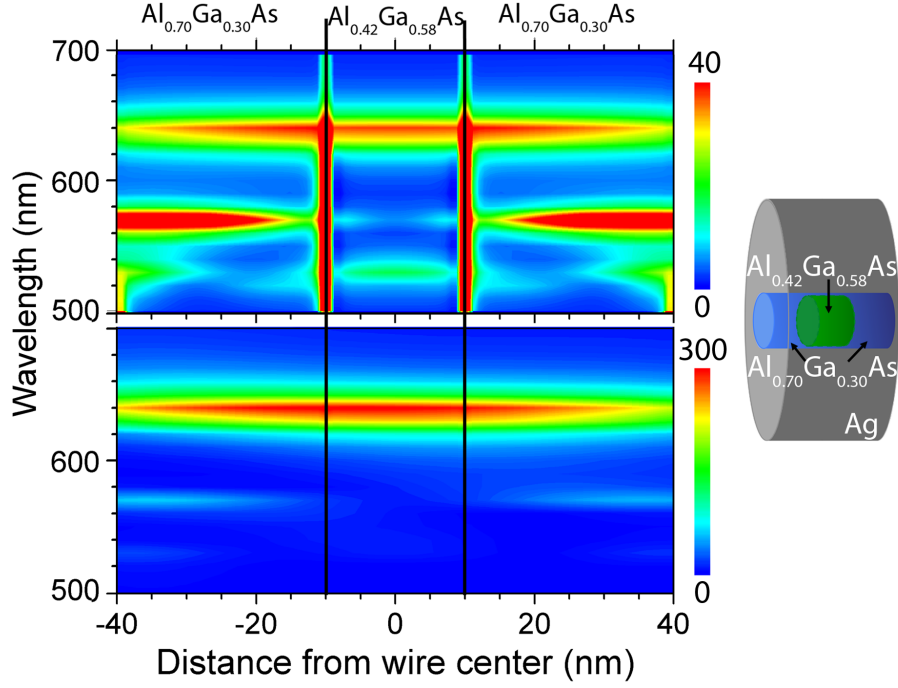


Figure 6.4. LDOS (top) and NF $|\mathbf{E}|^2$ (bottom) profiles showing the resonant modes for a structure with $\text{Al}_{0.42}\text{Ga}_{0.58}\text{As}$ active layer ($a = 15$ nm, $L_A = 20$ nm), $\text{Al}_{0.70}\text{Ga}_{0.30}\text{As}$ cladding ($s = 5$ nm, $L_C = 30$ nm), and Ag coating ($T = 100$ nm). The LDOS and NF $|\mathbf{E}|^2$ are calculated at a constant radial position of $r = 5$ nm from the center of the resonator core, and reported values of LDOS and NF $|\mathbf{E}|^2$ are normalized to the LDOS in vacuum and fields of the incident plane-wave source, respectively.

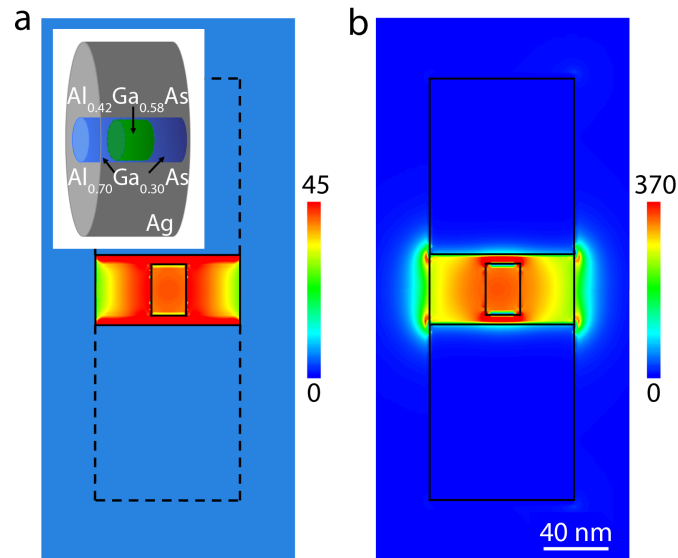


Figure 6.5. Two-dimensional (a) LDOS and (b) NF $|\mathbf{E}|^2$ cross sections of a core-shell nanowire resonator with $\text{Al}_{0.42}\text{Ga}_{0.58}\text{As}$ active layer ($a = 15$ nm, $L_A = 20$ nm), $\text{Al}_{0.70}\text{Ga}_{0.30}\text{As}$ cladding ($s = 5$ nm, $L_C = 30$ nm), and Ag coating ($T = 100$ nm). The LDOS is calculated at $\lambda = 637$ nm, the emission wavelength of the $\text{Al}_{0.42}\text{Ga}_{0.58}\text{As}$. The NF $|\mathbf{E}|^2$ cross section is calculated for plane-wave excitation at $\lambda = 637$ nm ($\theta = 0^\circ$).

6.3.3 In_{0.15}Ga_{0.85}N-GaN-Ag Resonator

Next, we consider as our active layer a 2 nm In_{0.15}Ga_{0.85}N single quantum well (SQW), with GaN as the cladding. Excitons in the In_{0.15}Ga_{0.85}N are highly localized, and therefore an explicit spacer layer is not modeled in this structure. The In_{0.15}Ga_{0.85}N quantum well emits at $\lambda = 440$ nm, and the resonator with the lowest-order longitudinal resonance at this wavelength has dimensions of $a = 5$ nm, $L_A = 2$ nm, $L_C = 10$ nm, and $T = 50$ nm. In this deeply subwavelength resonator, only extremely evanescent modes are supported. The LDOS and NF $|\mathbf{E}|^2$ for plane-wave excitation at $\theta = 0^\circ$ along the length of the wire are shown in Figure 6.6. At $\lambda = 440$ nm, the peak LDOS within the In_{0.15}Ga_{0.85}N SQW has a peak value of 900, more than twenty times the peak LDOS of the GaAs and Al_{0.42}Ga_{0.58}As resonators.

The two-dimensional LDOS and NF $|\mathbf{E}|^2$ cross sections in Figure 6.7 illustrate the high level of confinement within the core of this deeply subwavelength structure. Although the highest LDOS is seen at the semiconductor/metal interface, LDOS > 1000 is seen throughout the InGaN SQW. Furthermore, a peak electric field intensity of 3000 times larger than the incident plane wave is seen in Figure 6.7. This highest LDOS and NF $|\mathbf{E}|^2$ of the three resonators studied in detail here is achieved with the smallest resonator volume. We calculate $Q = 32$ and $V_{\text{eff}} = 4.3 \times 10^{-4}(\lambda/n)^3$, and find the highest Q/V_{eff} in this ultra-small resonator at $7.4 \times 10^4(\lambda/n)^{-3}$. Dramatic decay rate enhancements are found for this ultra-small structure, with $\Gamma_{\text{tot}}/\Gamma_0 = 8200$, $\Gamma_{\text{rad}}/\Gamma_0 = 3500$, and $\eta = 0.43$, which exceeds the radiative decay rate enhancements reported for metal nanoparticle structures [91]. This demonstrates that upon the transition from subwavelength resonators that support eigenmodes with sizable retardation effects to ultra-small resonators that support highly evanescent modes of a non-retarded nature, plasmonic core-shell nanowire resonators with dimensions on the order of $\lambda/50$ are able to strongly confine modes within the semiconductor core and to achieve dramatic enhancements in the radiative emission rate.

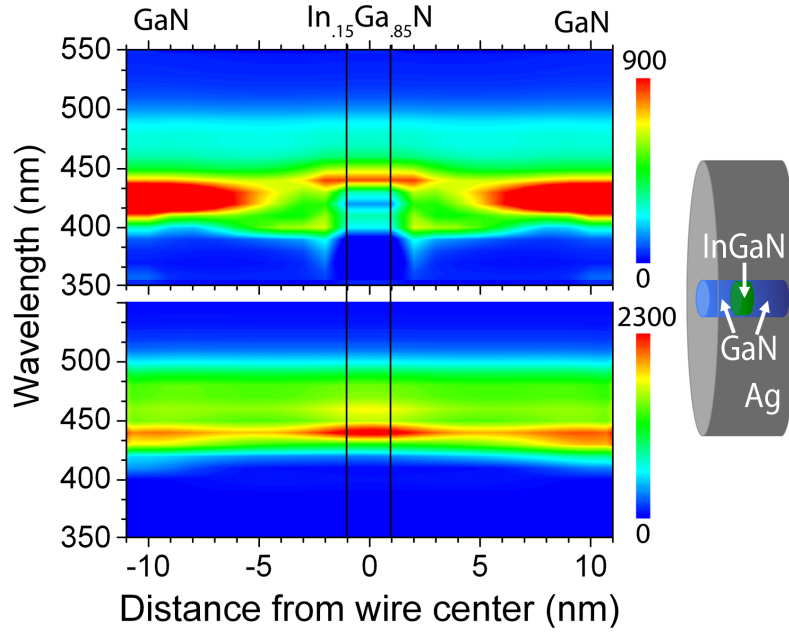


Figure 6.6. (top) LDOS (normalized to LDOS in vacuum) and (bottom) NF $|\mathbf{E}|^2$ for plane-wave excitation at $\lambda = 440$ nm, $\theta = 0^\circ$ (normalized to incident source) versus wavelength for a structure with $\text{In}_{0.15}\text{Ga}_{0.85}\text{N}$ active layer ($a = 5$ nm, $L_A = 2$ nm), GaN cladding ($L_C = 10$ nm and no spacer layer), and Ag coating ($T = 50$ nm). LDOS and NF $|\mathbf{E}|^2$ are calculated at a radial position of $r = 1$ nm from the center of the resonator core and along the longitudinal axis. Schematic of this structure is shown on the right.

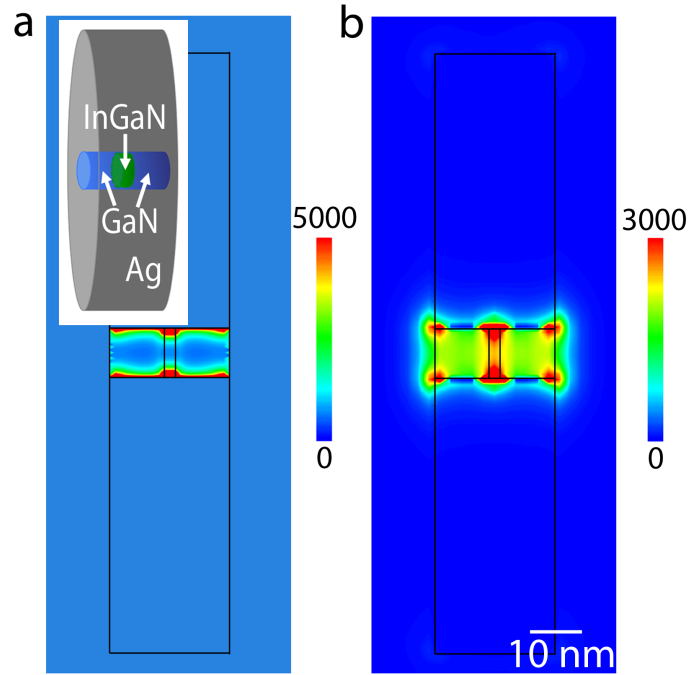


Figure 6.7. Cross-sectional (a) LDOS and (b) NF $|E|^2$ profile for a structure with $\text{In}_{0.15}\text{Ga}_{0.85}\text{N}$ active layer ($a = 5$ nm, $L_A = 2$ nm), GaN cladding ($L_C = 10$ nm and no spacer layer), and Ag coating ($T = 50$ nm). The LDOS is calculated at $\lambda = 440$ nm, the emission wavelength of the $\text{In}_{0.15}\text{Ga}_{0.85}\text{N}$ single quantum well. The NF $|E|^2$ is calculated for plane-wave excitation at $\lambda = 440$ nm ($\theta = 0^\circ$).

6.4 Enhanced Radiative Decay

The total decay rate enhancements and corresponding quantum efficiencies are plotted in Figure 6.8. Peaks in the plot of $\Gamma_{\text{tot}}/\Gamma_0$ versus wavelength correspond to the resonant modes illustrated in the LDOS plots of Figures 6.2, 6.4, and 6.6. The largest decay rate enhancements are seen for the $\lambda = 440$ nm mode of the ultra-small $\text{In}_{0.15}\text{Ga}_{0.85}\text{N}$ resonator, although significant enhancements are also observed for the GaAs and $\text{Al}_{0.42}\text{Ga}_{0.58}\text{As}$ resonators. Additionally, the quantum efficiencies η at the wavelengths of interest are $>50\%$ for these two resonators. Remarkably, even the smallest resonator ($\text{In}_{0.15}\text{Ga}_{0.85}\text{N}$ SQW) maintains a reasonable quantum efficiency of $>40\%$, suggesting that a large portion of the enhanced decay rate correlates to observable photons. The colored shaded regions on the graph correspond to a typical LED bandwidth centered at the emission wavelength of the active material, and because of the moderate quality factors in these plasmonic resonators, the rate of spontaneous emission is enhanced significantly throughout the entire band.

Finally, we also calculate the polarization dependence of the far-field (FF) radiation at the emission wavelength of each III-V semiconductor plasmonic core-shell nanowire resonators, and compare that to the emission polarization from an uncoated wire (GaAs active region with $a = 36$ nm, $L_A = 100$ nm, $\text{In}_{0.51}\text{Ga}_{0.49}\text{P}$ cladding and spacer with $s = 6$ nm and $L_C = 25$ nm, and no Ag coating). The polar plot is seen in Figure 6.9 for an observer looking down a radial axis. The FF radiation is determined for dipole excitation in the center of the resonator core, and the emission is isotropically averaged for all three dipole orientations (x , y , and z). The uncoated wire has a dipolar emission pattern oriented transverse to the longitudinal axis of the nanowire. Although not plotted here, the uncoated $\text{In}_{0.15}\text{Ga}_{0.85}\text{N}/\text{GaN}$ and $\text{Al}_{0.42}\text{Ga}_{0.58}\text{As}/\text{Al}_{0.70}\text{Ga}_{0.30}\text{As}$ wires show the same dipolar radiation pattern. With the Ag coating, all three of the resonators have a strongly modified emission polarization that is now oriented parallel to the longitudinal axis of the resonator. Dielectric materials tend to trap electromagnetic fields, so the z dipole in the uncoated GaAs nanowire is more efficient at polarizing the dielectric, and therefore emission is peaked

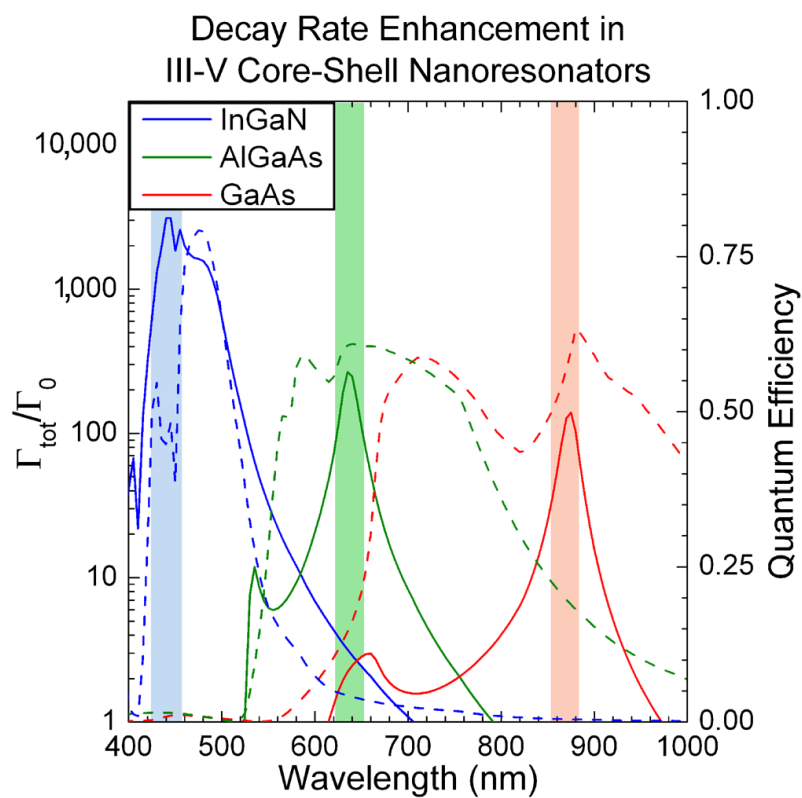


Figure 6.8. Total decay rate enhancement (solid) and quantum efficiencies (dashed) as a function of wavelength for the three different III-V core-shell nanoresonators. Colored shaded regions indicate typical spectral width of LED emission.

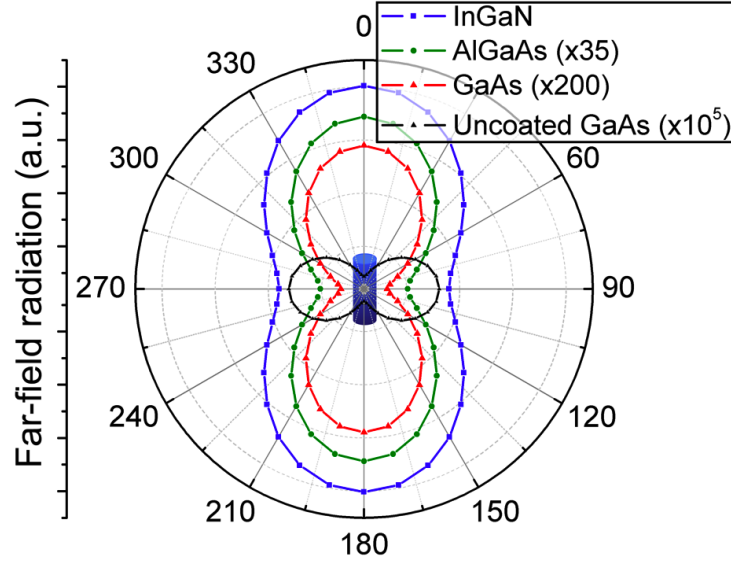


Figure 6.9. Polar plot of far-field radiation from dipole excitation of the same three core-shell nanoresonators (AlGaAs scaled $\times 35$, GaAs scaled $\times 200$) and in black a bare (uncoated, no Ag) GaAs/In_{0.51}Ga_{0.49}P nanowire (scaled $\times 10^5$). The Ag coating modifies both the intensity and direction of the far-field emission.

toward $\theta = 90^\circ$. In contrast, the metal coating quenches the z dipole, whereas radial dipoles couple naturally to modes of the metal-dielectric interface and dominate the resulting polar emission. Thus, the plasmonic coating modifies not only the rate of spontaneous emission but also the direction of far-field radiation.

6.5 Chapter Summary

In summary, we have introduced the III-V semiconductor plasmonic core-shell nanowire resonator geometry and shown that it is suitable for achieving dramatic enhancements in the rate of spontaneous decay of a variety of III-V materials, namely GaAs, Al_{0.42}Ga_{0.58}As, and In_{0.15}Ga_{0.85}N. In all three structures, the dimensions are chosen such that the lowest-order longitudinal resonance occurs at the band-edge emission wavelength of the active material, and the electric fields are highly confined within

Table 6.1. Summary of Q/V and decay rate enhancements in III-V semiconductor plasmonic core-shell nanowire resonators

active material	GaAs	Al _{0.42} Ga _{0.58} As	In _{0.15} Ga _{0.85} N
radius a (nm)	36	14	5
length L_A (nm)	100 (GaAs)	20 (Al _{0.42} Ga _{0.58} As)	2 (In _{0.15} Ga _{0.85} N)
length L_C (nm)	25 (In _{0.51} Ga _{0.49} P)	30 (Al _{0.70} Ga _{0.30} As)	10 (GaN)
spacer s (nm)	6 (In _{0.51} Ga _{0.49} P)	4 (Al _{0.70} Ga _{0.30} As)	0
Ag thickness T (nm)	100	100	50
λ (nm)	870	637	440
V_{eff}	$0.070(\lambda/n)^3$	$0.021(\lambda/n)^3$	$4.3 \times 10^{-4}(\lambda/n)^3$
Q	45	30	32
Q/V_{eff}	$645(\lambda/n)^{-3}$	$1435(\lambda/n)^{-3}$	$74000(\lambda/n)^{-3}$
$\Gamma_{\text{rad}}/\Gamma_0$	128	280	8,200
$\Gamma_{\text{tot}}/\Gamma_0$	223	460	3,500
η	57%	60%	43%

the resonator core. The increased LDOS due to the plasmonic coating contributes directly to enhanced spontaneous emission, and total decay rate enhancements of >8000 with quantum efficiency of $>40\%$ are observed for a structure with dimensions on the order of $\lambda/50$. Additionally, $Q/V > 10^4(\lambda/n)^{-3}$ was calculated, a value competitive with conventional high-Q dielectric microcavities. The numerical results are summarized in Table 6.1. We anticipate that as we continue to shrink resonator dimensions and incorporate new active materials that emit near the surface plasmon resonance, even higher LDOS and radiative decay rate enhancements will be achievable. This work demonstrates that III-V semiconductor plasmonic core-shell nanoresonators are a promising design for fast, bright, nanoscale, and perhaps even directional on-chip light sources.